Z_1 oscillations in yields of multicharged ions emitted from a germanium surface when bombarded by light ions

B. Hird, R. Armstrong, and P. Gauthier
Ottawa-Carleton Institute for Physics, Ottawa University Campus, Ottawa, Ontario, Canada K1N 6N5
(Received 18 August 1994)

The interaction radii at which holes are created in the L shell of light projectiles and in the M shell of germanium during ion–surface-atom collisions have been determined from the thresholds for doubly charged ion production. In contrast to the data with a silicon target, the interaction radius at which electron promotion occurs does not decrease with projectile atomic number Z_1, as it should if promotion occurs at a definite level crossing. In addition, the yields of doubly charged ions do not follow the Z_1 dependence predicted by the Fano-Lichten electron-promotion model [Phys. Rev. Lett. **14**, 627 (1965)].

PACS number(s): 79.20.Rf, 34.70.+e

I. INTRODUCTION

When ions of a few keV energy are scattered from surfaces, it has been found that there are significant differences in the proportions of different charge states of scattered and recoiled target ions, when compared to similar measurements with low pressure gases [1,2]. It seems likely that the multicharged ions originate in the same ion-atom close encounters as in ion-gas collisions but, once produced, the collective behavior of the other atoms in the solid influences the charge of these ions by neutralization. We report measurements of the yields of doubly and singly charged ions which are scattered and recoiled from a clean amorphous germanium target when bombarded with C^+, N^+, O^+, F^+, Ne^+, Na^+, P^+, S^+, Cl^+, and Ar^+ ions of a few keV energy. Previously we reported similar measurements with a silicon target [3]. The situation is quite different from the equilibrium charge states produced when MeV ions are transmitted through thin foils since the average charge state after passing through a foil is higher than through an equivalent thickness of gas [4], whereas keV ions scattered from a solid produce correspondingly fewer multicharged ions than in ion-gas scattering.

The last stages in the production of multicharged ions are mainly Auger transitions in which the excitation energy of the ion is in part converted to ionization energy of one or more valence electrons, thus increasing the charge state. The excited state which emits the Auger electrons may have inner-shell vacancies, or they may have already been filled, and some of the excitation energy transferred to outer shells. However, the excitation must have been created earlier in the same collision and is likely to have been initiated by the electron-promotion process [5,6], which produced one or more inner-shell vacancies.

A characteristic of inner-shell electron promotion is that it predominantly occurs at specific level crossings in the correlation diagram of the ion-atom molecular orbitals. These level crossings must be traversed during the collision, otherwise electron promotion is unlikely. For the production of K-shell and L-shell vacancies, the important level crossings occur at interaction distances less than 1 a.u. These distances are significantly smaller than the separation between the atoms in a solid. For example, the nearest-neighbor separation in a germanium crystal is 4.63 a.u. The inner-shell vacancies are thus produced only in violent close ion-atom encounters in which the distance of closest approach during the collision is much less than the separation between atoms in the solid. The presence of neighboring atoms several a.u. away, and therefore also all the other properties of the solid, should thus not significantly affect this first step in the multicharged ion production process. In contrast, the later interactions as the ions leave the surface account for the differences between ion-gas and ion-surface scattering. These include (a) the decay of outer-shell or valence electrons to fill these vacancies, (b) Auger transitions which increase the ionization state of the ions, and (c) capture of electrons from the solid, which reduce the ionization state. The relative importance of each of these processes is uncertain, and it is not clear where, with respect to the solid surface, the final charge of the ion is determined.

Other measurements that give related information on these processes are x-ray yields following high energy ion-solid collisions and electron spectroscopy of surfaces bombarded with ions in which characteristic Auger electrons are identified. Large oscillations have been reported by Kavanagh *et al.* [7,8] in the Cu x-ray yields as a function of the projectile atomic number (Z_1). They established that the maxima occur when the shell energies of the target and projectile ions match, as previously found in ion-gas collisions [9]. Their measurements were done at low enough energy for the molecular orbital model to be valid, but at high enough energy for backward scattering ion trajectories to reach the level crossings which promote electrons from the K shell of the lighter element. They found a maximum near $Z_1 = 32$, where the target and projectile L-shell energies match, and a second maximum near Ne whose K-shell binding energy is close to the L-shell binding energy of Cu. The positions of both

these maxima were invariant to the collision energy. No similar systematic investigation of Auger electron yields with low energy ions has been reported; however, the emission of L-shell Ar^+ Auger electrons was found to decrease with increasing atomic number for targets from $Z_2 = 20$ to $Z_2 = 29$ [10], as would be expected from the increasing difference between the target and projectile L-shell binding energies.

Measurements of the mean charge of ions transmitted through carbon foils [11] have also shown an oscillation in the light elements, with a maximum near $Z_1 = 17$ [12]. These measurements were made at high energies where the molecular orbital model is probably not valid, so that electron promotion at level crossings may not dominate and multiple ionization may be produced by direct excitation rather than by Auger processes. However, the results again seem to be in agreement with shell matching, in that the peak in the mean charge occurs where the binding energy of the target $2s$ shell matches the K-shell binding energy of carbon.

While these processes have provided information on the way in which inner-shell vacancy production varies with Z_1 and Z_2, it is difficult to relate the x-ray yields and the Auger electrons to specific ion trajectories because both are emitted nearly isotropically in the frame of the moving ion, so that apart from small Doppler shifts, the directional information about the particular ion trajectories which produced the shell vacancies is not determined experimentally and must be inferred from a theoretical model. The present measurements determine the electron promotion level crossing radii in a very direct way. The incident and emitted ion energies and directions are well defined so that the ion–surface-atom trajectories can be calculated using a screened Coulomb potential. At a fixed scattering angle the distance of closest approach decreases as the beam energy is increased. When it reaches the radius for electron promotion, multiply charged ions first appear in the spectrum. Thus measurements of the energy thresholds for multiply charged ion production determine directly the crossing radii for electron promotion. Although obtained by a very different method, there is reasonable agreement with crossing radii derived from ion-gas Auger electron cross section measurements. In the one case where the same beam target has been measured both ways, Schneider *et al.* [13] found a value of $r_0 = 0.65$ a.u. from the Si^+-Ar Auger cross section, while a value of $r_0 = 0.72 \pm 0.02$ a.u. was found from the Si^{2+} threshold in Ar^+-Si surface scattering [3].

The ion-atom trajectories were calculated using the "universal" screened Coulomb potential of O'Connor and Biersack [14]. We have found that this potential, which has no adjustable parameters, gives essentially identical results, when used for light ions at a few keV energy, to the Ziegler-Biersack-Littmark [15] potential in which the screening length is adjusted empirically to match experimental shadow cone data [16].

The multicharged ion yields are influenced by many processes including shadowing, blocking, and surface neutralizing interactions as these ions escape from the solid, so that a detailed interpretation is difficult. The energy thresholds, in contrast, should be independent of such processes and depend only on the initial close encounter region of the ion-atom trajectories.

II. EXPERIMENT

The instrumental requirements for low energy ion scattering measurements using an electrostatic analyzer system has been described in previous publications [17,18]. The beams were produced using pure gases (N_2, O_2, Ne, and Ar) in a discharge-type ion source. C^+, F^+, and Cl^+ beams were produced with CO, Freon-14 (CF_4) and Freon-12 gas (CCl_2F_2), respectively, whereas P^+, S^+, and Na^+ beams were obtained by placing small amounts of the element in solid form inside the ion source while operating the plasma on argon gas. The ions of the most common isotope of each element were selected with a high resolution 30° deflection magnet. The beam passed through a differentially pumped section between two small apertures which both defined the beam geometry and isolated the scattering chamber, allowing a pressure of 2×10^{-10} Torr during measurements. The target was a Ge(100) crystal with its surface amorphized and cleaned by 500-eV Ar^+ bombardment. Following each sputtering, the target was heated to about 500 °C for 10 s, during which time the pressure rose due to desorption of the absorbed argon and then returned almost to the pressure before heating. An amorphous surface was chosen for the measurements so as to avoid any uncertain crystallographic effects from a single crystal surface damaged by the ion beam. Crystal damage by the beam was produced much faster than the buildup of surface impurities, so that it was possible to use the amorphized surface longer before it required recleaning. At a few keV beam energy the background from subsurface scattering was only slightly larger than from a single crystal with ions incident along a channeling direction.

The scattered and recoiled ions that were emitted from the target were energy and charge state analyzed by a $\pi/\sqrt{2}$ electrostatic spectrometer located on a moveable platform inside the scattering chamber. A typical voltage spectrum of the ions emitted at 45° to the incident oxygen beam direction is shown in Fig. 1. The voltages, at which the peaks appear, all agree with the energies expected from events in which an incident O^+ ion is either scattered out from the surface after colliding with a single germanium atom or scattered inward at an angle close to 78°, and the germanium ion recoils outward at 45°. The scattering angles were judiciously chosen for optimum separation of the singly and doubly charged ion peaks of both scattered and recoiled particles. At higher energies, multiple scattering processes produced shoulders on the high voltage side of the single collision peaks. However, at a few keV beam energy, these contributed insignificantly to the ion yields. To within the resolution of the analyzer, all the multicharged ions had the same energy as the singly charged ions, since the doubly charged ion peaks occur, to within one channel, at exactly half the voltage of the corresponding singly charged ion peak. This 1:2 voltage ratio did not vary when the scattering angle was changed, eliminating the possibility that the

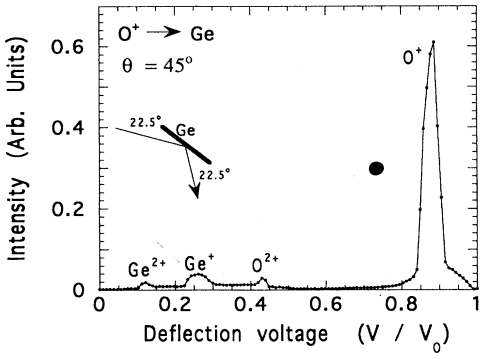

FIG. 1. Electrostatic analyzer spectrum of ions which have been scattered though an angle of 45° by a clean amorphous germanium surface. V is the analyzer deflection voltage and V_0 is the voltage required to deflect the full energy incident beam. The scattered and recoil singly charged ions appear at the predicted binary collision energies. The doubly charged ions always appear at exactly half the voltage of the corresponding singly charged ions.

peaks which we interpret as multicharged ions might be singly charged scattered or recoiled ions from surface contaminants. No triply charged ions were observed for the germanium target, although significant Si^{3+} yields had been found previously with a silicon target [3].

III. RESULTS

A. Variation with beam energy

Figure 2 shows a typical variation of the scattered ion intensity with beam energy and Fig. 3 shows the corresponding yields of recoiling germanium target atoms which escape from the surface as singly and doubly charged ions. Intensities were determined from the areas under the elastically scattered ion peaks and the background from subsurface scattering was subtracted by linear interpolating the counts on each side of the peak. It was not possible to obtain absolute yields because of difficulties in normalizing the ion counts to a known beam charge. The beam intensities, typically 10^{-9} A, were too small to be measured accurately with a picoammeter, whose amplifiers are too slow to follow the short term beam fluctuations. As an estimate of the beam intensity, a channel electron multiplier (CEM), mounted behind a small pinhole aperture, counted all the particles of all energies which were emitted at close to 180° to the incident ion direction. Each channel count of the spectrometer was normalized to these CEM counts, taken during the same time interval. The spectra, normalized in this way, were accurately reproducible and substantially independent of the beam intensity. This normalization procedure is valid when the energy and the angle of the target are held constant, but there may be some energy variation of the total yield of backscattered ions. These normalization problems are not present in the relative yields of different charge states.

The general shape of the yields as a function of beam energy will probably be affected by shadowing effects. The ions are incident on the germanium surface at an angle of 10° and detected at 30° with respect to the surface, for a total scattering angle of 40°. At these small incident angles not all the surface-atoms are visible to the incoming beam because some lie within the shadow cone of neighboring atoms on the surface. At a separation of 7.6 a.u., which is the surface-atom separation on a (100) crystal and can reasonably be assumed to be the average separation on an amorphous surface, the shadow cone angle is 12° for 10-keV oxygen ions. This shadow cone angle decreases with energy and increases with Z_1, so that the shadow cones will be less than 12° for higher energies and lighter projectiles. The observed ion yields are thus reduced by surface shadowing effects mostly at our lowest energies and with heavier projectiles.

The shadowing effects are expected to be nearly the same for all charge states of the emitted ions and should cancel out in the ratio of yields [Figs. 2(c) and 3(c)]. Neutralization and Auger ionization, which mainly determine the final charge state after the ion direction has

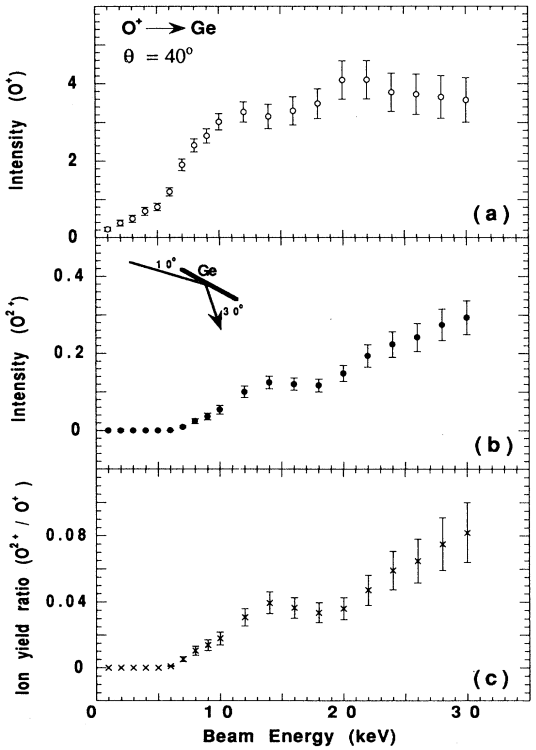

FIG. 2. Yields of (a) O^+ and (b) O^{2+} ions which have been scattered through an angle of 40° by collisions with surface or near surface atoms, as a function of the incident O^+ ion energy. The yields are normalized to the count in a CEM which detected ions of all energies emitted at a backward direction. The ratio of doubly charged to singly charged scattered ions is shown in (c). The same normalization was used for both yields, so that (c) shows the absolute ratio of the numbers of these ions, which are emitted at 30° to the surface.

been changed at the close encounter, occur during the outgoing part of the trajectory. The ion trajectories are thus expected to be very similar for ions of all charge states which have been deflected by the same scattering angle. The situation is less clear for blocking. If the final charge state is influenced by how closely the trajectories have passed to neighboring atoms, then there may be charge-dependent blocking cone effects. A comparatively large exit angle of 30° was therefore chosen to minimize the effects of blocking in the present measurements.

B. Scattered ion yields

The yields of singly and doubly charged scattered ions for various incident ions are shown in Fig. 4. Measurements were made at a constant ion beam velocity so as to minimize the changes to the yields due to kinematic variations. A velocity of 0.53 keV/amu was chosen as a compromise, to be well above the energy thresholds for doubly charged ion production, but low enough to avoid significant subsurface and multiple scattering contributions to the binary collision peaks.

The singly charged scattered ion yield increases from a small value for C^+, to a large value for Na^+, returning to small values for P^+, S^+, and Cl^+ with some indication

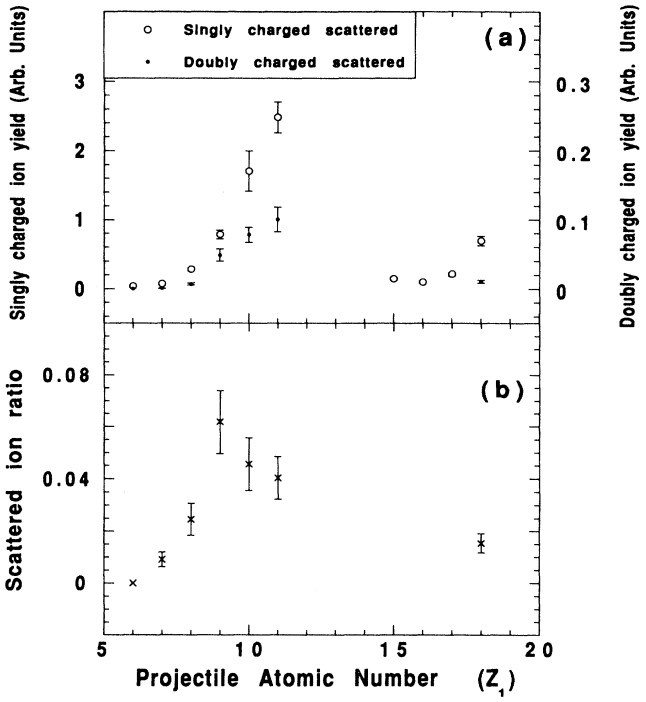

FIG. 4. Yields of singly and doubly charged scattered ions as a function of the atomic number Z_1 of the incident beam (a). Open circles are singly charged ions and dots are doubly charged ions. The absolute ratio of doubly to singly charged scattered ions is shown in (b).

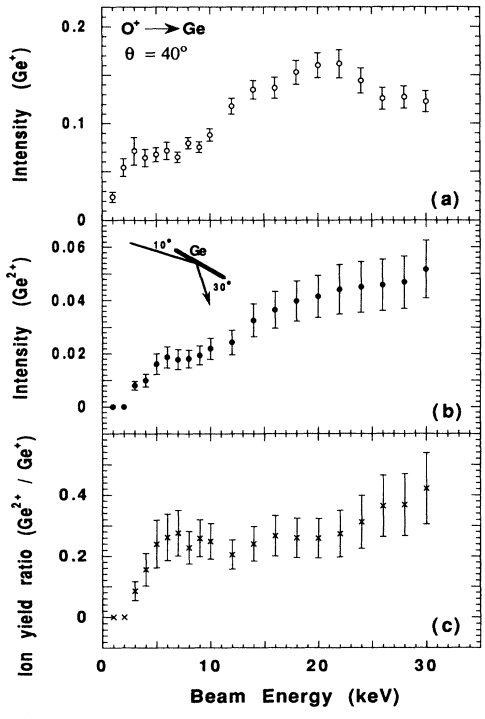

FIG. 3. Yields of (a) Ge^+ and (b) Ge^{2+} ions which have recoiled at 40° to the incident ion direction from surface or near surface locations (oxygen ions scattered inwards at 87°), plotted as a function of the incident O^+ ion energy. The absolute ratio of Ge^+ to Ge^{2+} ions is shown in (c).

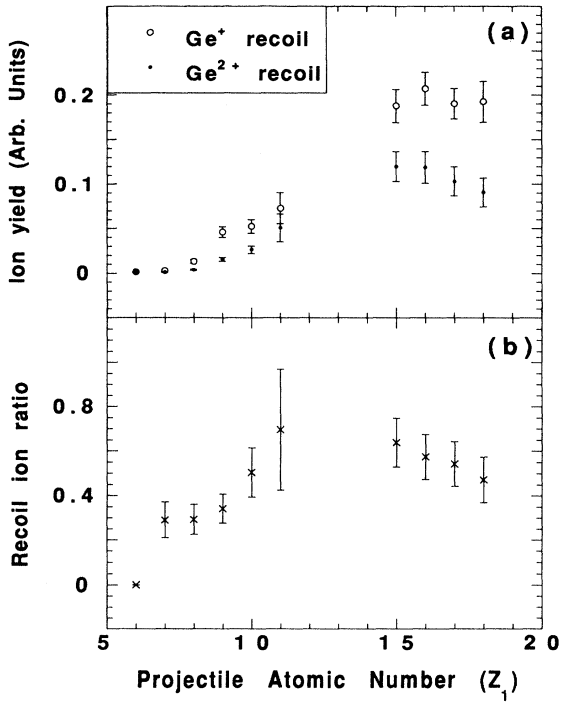

FIG. 5. Yields of Ge^{2+} and Ge^+ ions emitted at 40° to the incident ion direction, as a function of the atomic number Z_1 of the incident beam (a). Open circles are singly charged ions and dots are doubly charged ions. The absolute ratio of doubly to singly charge scattered ions is shown in (b).

of an increase for Ar^+. The doubly charged scattered ion yield shows a similar behavior, with a rise from undetectably low values for C^{2+} to significant values for F^{2+}, Ne^{2+}, and Na^{2+}. The yield then returns to an undetectably small value for P^{2+}, with a small increase for higher Z_1 ions. The ratio of yields therefore shows a maximum in the region $Z_1 = 9 - 11$, with very small ratios elsewhere.

C. Recoil ion yields

The yields of Ge^{2+} ions and Ge^+ ions emitted from the target at 40° to the incident beam are shown in Fig. 5. Both singly and doubly charged recoiled ion yields increase from $Z_1 = 6$ to $Z_1 = 11$, as occurs for the scattered ions. For $Z_1 < 14$, both the Ge^+ and the Ge^{2+} yields are much smaller than the corresponding scattered ion yields. For $Z_1 > 14$, where the scattered ion yields are undetectably small, significant Ge^+ and Ge^{2+} yields were found. Both recoiled ion yields appear to go through a broad maximum.

Because of the more nearly equal recoiled ion yields, the absolute ratio could be determined for all the ion beams. The ratio may be an oscillatory function of Z_1 with a maximum in the region between $Z_1 = 11$ and $Z_1 = 15$, which is not accessible to us.

IV. CROSSING RADII

Definite energy thresholds were found for all the doubly charged ions. As the beam energy is increased, for a fixed scattering geometry, the distance of closest approach during the collision between the incident ion and an atom in the target decreases. An energy threshold therefore occurs where this distance equals the crossing radius in the molecular orbital correlation diagram at which electron promotion occurs to create shell vacancies. These crossing radii may thus be calculated directly from the threshold energy. The Ge^{2+} threshold can be similarly calculated because target atoms which recoil in a definite direction correspond to definite scattering trajectories.

The energy thresholds for the appearance of doubly charged scattered and recoiled ions are shown in Table I and in Fig. 6. They were determined experimentally by decreasing the beam energy in small steps until the region of the spectrum where the doubly charged peak was expected showed no statistical count above background. This method provided a consistent and reproducible energy value, but it is possible that somewhat larger crossing radii values would be obtained in an experimental system which was able to detect smaller intensities of doubly charged ions.

The scattered and recoiled r_0 values show distinctly different behavior. However, in both there is a clear discontinuity in trends of the data between $Z_1 = 11$ and $Z_1 = 15$. In x-ray and Auger electron data such changes are associated with level matching. It is well established from ion-gas experiments [19,20] that in nearly symmetric collisions, K-shell holes are mostly formed in the lower Z partner, so that mostly projectile holes occur when $Z_1 < Z_2$ and mostly target holes when $Z_1 > Z_2$. In terms of the correlation diagram, the change is associated with level swapping on either side of $Z_1 = Z_2$, with electrons in the higher energy orbital being promoted. A similar level matching between different shells is also possible for collisions with very dissimilar Z_1 and Z_2. The atomic shell energies suggest that the matching occurs between the M shell of Ge and the L shell of the projectile, which should cross at about $Z_1 = 14$. Figure 7 shows the united atom and separated atom limits of the correlation diagrams for collision pairs on either side of this level match. In the Fano-Lichten [5] molecular orbital electron-promotion model, as described by Barat and Lichten [6], the $4d\sigma$-$4f\sigma$ promoted electrons come from the $2p$-$2s$ shell of Na. In contrast, on the higher Z_1 side of the M-L shell match, because of level swapping, these same orbitals promote the $3p$-$3d$ electrons from Ge.

In the x-ray yields from Cu [7,8] two clear systematic trends are associated with level matching. First there is a variation of $\sim 10^3$ in the total x-ray yield, depending on how close the energy levels are to the match, and second the yield changes from being mostly projectile x rays on the lower Z_1 side of the match to mostly target

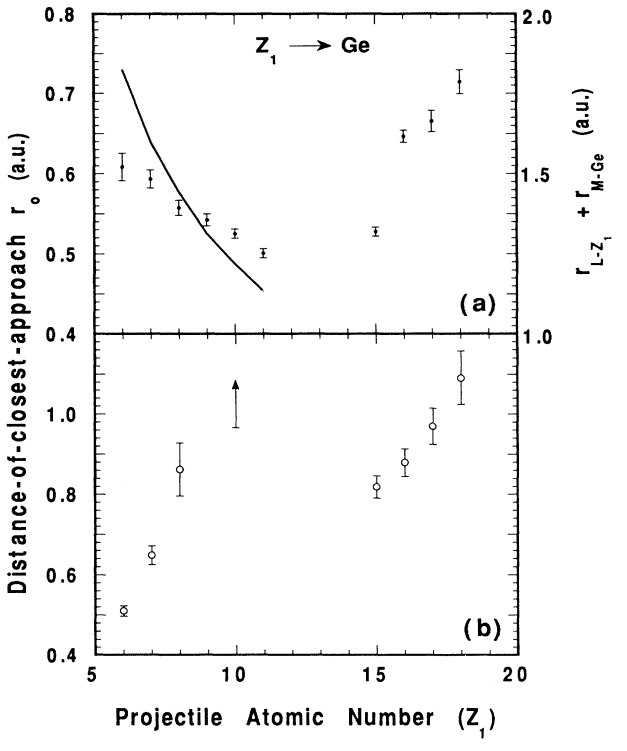

FIG. 6. The distance of closest approach r_0 during binary surface collisions for the lowest beam energy at which doubly charged ions were detected. This distance is associated with the crossing radius for electron promotion in the molecular orbital correlation diagram. The r_0 values are shown as a function of the beam atomic number Z_1 (a) for scattered doubly charged ions and (b) for recoil Ge^{2+} ions.

TABLE I. Energy thresholds E_t, and distances of closest approach r_0, calculated with the "universal" screened Coulomb potential of O'Connor and Biersack [14]. θ is the angle between the incident ion direction and the detected ion direction. θ' is the scattering angle when recoil Ge^{2+} ions are detected at θ.

Beam	θ	θ'	Scattered ions		Recoil Ge^{2+}	
			E_t (keV)	r_0 (a.u.)	E_t (keV)	r_0 (a.u.)
C^+	45°	80.6°	3.6 ± 0.2	0.609	3.4 ± 0.2	0.510
N^+	45°	79.1°	4.4 ± 0.1	0.593	2.3 ± 0.2	0.648
O^+	45°	77.6°	5.7 ± 0.1	0.558	1.1 ± 0.2	0.862
F^+	45°	75.3°	6.8 ± 0.1	0.542		
Ne^+	45°	74.6°	8.0 ± 0.1	0.525	< 1.0	> 1
Na^+	50°	63.5°	8.9 ± 0.1	0.500	2.7 ± 0.7	0.5
P^+	35°	84.8°	14.1 ± 0.1	0.527	2.3 ± 0.1[a]	0.818
S^+	35°	84.0°	9.4 ± 0.1	0.646	2.0 ± 0.1[b]	0.879
Cl^+	40°	72.2°	4.2 ± 0.1	0.665	1.2 ± 0.2	0.969
Ar^+	40°	69.1°	3.8 ± 0.1	0.714	1.2 ± 0.2	1.09

[a] $\theta = 40°$, $\theta' = 75.6°$.
[b] $\theta = 40°$, $\theta' = 74.8°$.

x rays on the higher Z_1 side. These trends are much less evident in the ion spectra. On the high side of the match there is a small increase in both the Ge^{2+} and Ge^+ ions and the doubly charged scattered ions were too few to be detected, with small yields of singly charged ions. On the lower Z_1 side of the match there is a slight increase in the yield of scattered ions, but a strong increase in the singly charged yield. These results suggest that most of the emitted singly charged ions are produced by level crossing processes and are not survivors of the singly charged ions of the incident beam [17]. An increased yield of singly charged ions would occur if there were increased hole production as the shell match is approached and most of the multicharged ions which result from the Auger transitions which fill the holes decay to singly charged ions as they pass out through the surface. Perhaps also the increasing neutralization with increasing Z_1 occurs because in this region the electron affinity is decreasing and the electrons are more easily captured by the emitted ions.

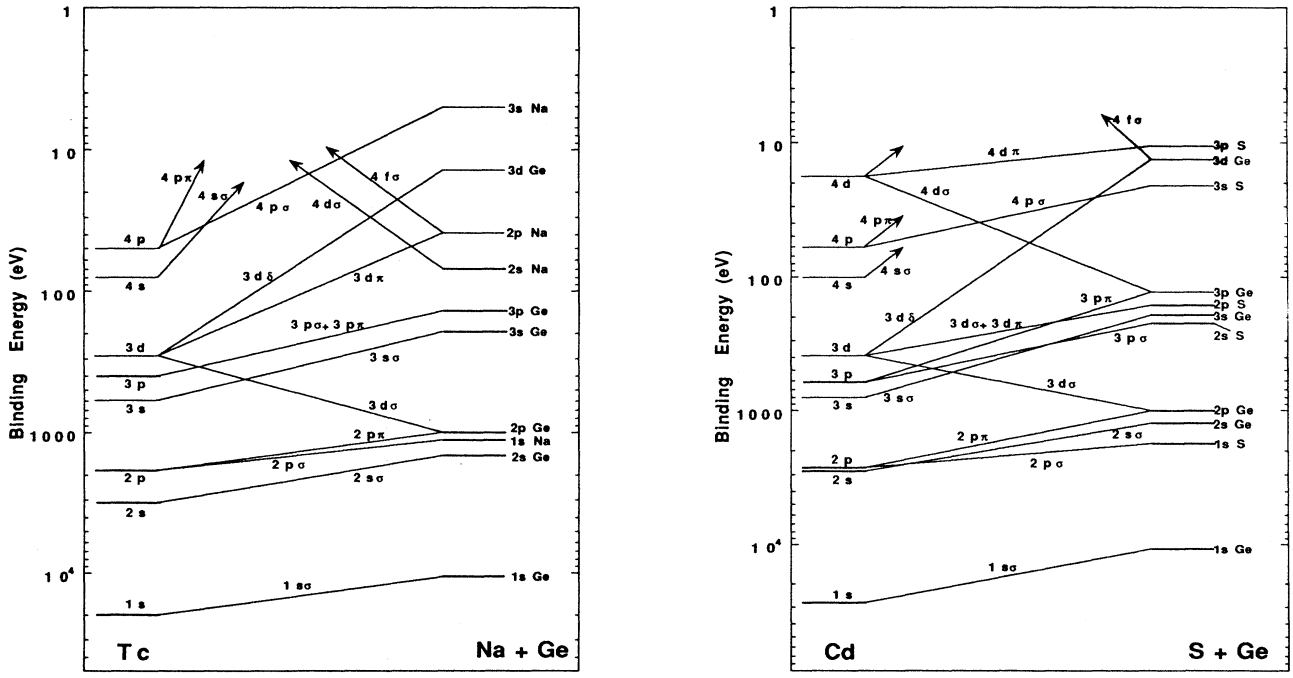

FIG. 7. The separate atom and united atom limits for the correlation diagrams of Na-Ge and S-Ge, showing the change in level ordering associated with swapping of the $4d\sigma$ and $4f\sigma$ molecular orbitals.

V. DISCUSSION

The increase in r_0 with Z_1 is hard to explain if electron promotion follows the correlation diagram closely. For a specific level crossing a decrease in r_0 is always expected from the generally decreasing size of each molecular orbit with increasing Coulomb charge. Detailed calculations of molecular orbitals support this [21], as do ion-gas energy loss measurement of K-shell hole formation systematics [19]. Previous measurements of the energy thresholds for doubly charged ion production with an amorphous silicon target [3] also observed this behavior, with decreasing values of r_0 from $Z_1 = 6$ to $Z_1 = 10$ and then higher but decreasing values from $Z_1 = 15$ to $Z_1 = 18$. This is exactly what was expected from the electron promotion model if there is a change in the orbit at or near the symmetric interaction with $Z_1 = Z_2 = 14$. Only for the scattered doubly charged ion production with the germanium target do we observe a decrease in r_0. The line in Fig. 6 shows the sum of the separated atom radii for the L shell of the projectile and the M shell of germanium. While the magnitude is not a good representation of the molecular orbital crossing radius, the Z_1 variation should be reasonably correct. However, the r_0 values appear to decrease less than the atomic radii.

The Z variations of x-ray yields [7–9] do not show a decrease, followed by a discontinuous rise at the Z_1 value where the correlation diagram predicts a change in the level crossing. Instead they are oscillatory, with a gradual rise to a maximum at the level match, suggesting that transitions at both level crossings occur with gradually changing probabilities. It is possible that our observed rising values of r_0 are in a region where promotion at more than one level crossing is important.

X-ray data cannot be compared directly with the present r_0 values without several approximations. A simple model has been used to derive r_0 values from the x-ray cross sections [22]. It assumes that there is a constant probability P that an electron hole is created in the shell when the trajectory has an impact parameter less than b_0 and that otherwise $P = 0$. The cross section for x-ray production can then be written

$$\sigma_x = P \pi b_0^2 \omega,$$

where ω is the fluorescent yield. The critical impact parameter b_0 occurs where the trajectory just reaches the crossing radius for electron promotion r_0. While an analytic relation exists between b_0 and r_0 for the Molière potential, the r_0 values can be more conveniently obtained by numerically integrating the trajectories.

The Ge^{2+} recoiled r_0 values should show the same general Z dependence as the x-ray data, with the maximum at approximately the same Z values, since the atomic number of copper ($Z_1 = 29$) is not very different from that of germanium ($Z_2 = 32$). A fluorescent yield value of $\omega = 0.0056$ was chosen by Kavanagh *et al.* [7,8] so as to match the r_0 values near the symmetric $Z = 29$ peak to the geometric size of the L shell of copper. This is a typical ω value [23]. However, when applied to the lower Z_1 targets of interest here, this value of ω predicts r_0 values which are unphysically small, of the order of the K shell radius. Barat and Lichten [6] obtained reasonable r_0 values from the Kavanagh *et al.* x-ray cross sections by multiplying the simple cross section formula by a probability factor which decreased with increasing Z on both sides of the cross section maximum. Their probability factor becomes very small when extrapolated outside its region of validity to our lower Z_1 projectiles.

Ignoring the discrepancy in the magnitudes and considering only the Z variation of r_0, the rise in our data from $Z_1 = 6$ to $Z_1 = 8$ can be associated with the rise to the maximum at about $Z_1 = 10$ in the x-ray data due to the L-M shell energy match. Also the rise from $Z_1 = 15$ to $Z_1 = 18$ may be the beginning of the rise to the L-L shell energy match in symmetric collisions. If this interpretation is correct, in both regions electron promotion occurs at a varying mixture of level crossings and involves more than one shell.

The similarity in the scattered and recoiled ion yields on either side of the M-L shell energy match is incompatible with the preferential ionization of the lower Z atom in nearly symmetric collisions, which is clearly established in ion-gas collisions, but here, in ion-surface collisions, has only a weak effect on the ratio on either side of the energy match. A two-electron process has been proposed by Stolterfoht [24] in which two holes in the orbit which corresponds to the higher energy shell are converted into one hole in the orbit for the lower energy shell. The process is a two-electron resonant transition in which the energy to promote one electron from the lower to the higher energy shell is obtained by the demotion of a second electron from a Rydberg state to fill the second hole. Stolterfoht proposed this to account for the production of Ar as well as Si Auger electrons in Ar^+-SiH_4 gas scattering. Although we found no detectable Ar^{2+} ions in previous Ar^+-Si surface scattering measurements [3], this process may account for the presence of both scattered and recoiled doubly charged ions in all of the present Ge measurements.

It would be necessary to make measurements over a wider range of Z_1 projectiles to establish whether there are level matching oscillations in the r_0 values comparable with those in x-ray yields. There may also be oscillations in the total ion yield, if electron promotion at level crossings is the main interaction process which initiates the complicated sequence of interactions by which most energetic ions, including singly charged ions, are produced following quasielastic ion–atom-surface collisions.

After the ions are initially formed and before they leave the surface, there is a significant probability that the charge will be reduced as the ion picks up electrons. The interactions that determine the decay rates probably depend on surface electronic properties such as the work function, the valence bandwidth, and the density of states at the surface. This complicates the interpretation of the ion yields, but should not affect significantly the determination of the crossing radii. There may also be surface structure effects when crystals are used. The yield of different charges may depend on how close the emitted ions pass to other surface atoms on their way out from the surface. Such effects would be observed as charge-dependent blocking cone angles.

[1] W. F. van der Weg and D. J. Bierman, Physica **44**, 177 (1969).
[2] S. Datz and C. Snoek, Phys. Rev. **134**, A347 (1964).
[3] B. Hird, R. A. Armstrong, and P. Gauthier, Nucl. Instrum. Methods **B90**, 243 (1994).
[4] H. D. Betz and L. Grodzins, Phys. Rev. Lett. **25**, 211 (1980).
[5] U. Fano and W. Lichten, Phys. Rev. Lett. **14**, 627 (1965).
[6] M. Barat and W. Lichten, Phys. Rev. A **6**, 211 (1972).
[7] T. M. Kavanagh, M. E. Cunningham, R. C. Der, R. J. Fortner, J. M. Khan, and E. J. Zharis, Phys. Rev. Lett. **25**, 1473 (1970).
[8] T. M. Kavanagh, R. C. Der, R. J. Fortner, and M. E. Cunningham, Phys. Rev. A **8**, 2322 (1973).
[9] F. W. Saris, Physica **52**, 290 (1971).
[10] F. Xu and A. Bonanno, Phys. Rev. B **46**, 11 405 (1992); Surf. Sci. Lett. **273**, L414 (1992); F. Xu, P. Riccardi, A. Oliva, and A. Bonanno, Nucl. Instrum. Methods B **78**, 251 (1993).
[11] W. N. Lennard and D. Phillips, Phys. Rev. Lett. **45**, 176 (1980).
[12] W. N. Lennard, T. E. Jackman, and D. Phillips, Phys. Rev. A **24**, 2809 (1981).
[13] D. Schneider, G. Nolte, U. Wille, and N. Stolterfoht, Phys. Rev. A **28**, 161 (1983).
[14] D. J. O'Connor and J. P. Biersack, Nucl. Instrum. Methods B **15**, 14 (1986).
[15] J. F. Ziegler, J. P. Biersack, and V. Littmark, *The Stopping and Range of Ions in Solids* (Pergamon, New York, 1985).
[16] H. Bu, M. Shi, and J. W. Rabalais, Nucl. Instrum. Methods B **61**, 337 (1991).
[17] B. Hird, R. A. Armstrong, and P. Gauthier, Phys. Rev. Lett. **67**, 3575 (1991).
[18] B. Hird, R. A. Armstrong, and P. Gauthier, Phys. Rev. A **49**, 1107 (1994).
[19] B. Fastrup, G. Herman, and K. J. Smith, Phys. Rev. A **3**, 1591 (1971).
[20] E. G. Bøving and G. Sørensen, Phys. Rev. Lett. **40**, 315 (1978).
[21] U. Wille and R. Hippler, Phys. Rep. **132**, 129 (1986).
[22] R. K. Cacak, Q. C. Kessel, and M. E. Rudd, Phys. Rev. A **2**, 1327 (1970).
[23] R. J. Fortner, Phys. Rev. A **10**, 2218 (1974).
[24] N. Stolterfoht, Phys. Rev. A **47**, R763 (1993).